COMMUNICATION

Check for updates

Synthesis of Bz-TTFs with polymerization sites and the properties of Li-ion batteries comprising them as active materials†

Aya Yoshimura, [ID] [a] Moeko Yoshinouchi,[a] Keisuke Hemmi,[a] Yuto Aso,[a] Ryosuke Utsumi,[a] Takashi Shirahata, [ID] [ab] Masaru Yao [ID] [c] and Yohji Misaki [ID] ★[ab]

Two benzene-fused tetrathiafulvalene compounds with polymerization sites as positive electrode materials were synthesized. The molecular structures were determined by single-crystal X-ray structure analysis, and electrochemical analysis confirmed the formation of the polymer on the electrode. One of the synthesized compounds exhibited a long cycle life and a high rate performance.

Owing to their high energy density, high discharge power, and long storage life, lithium-ion batteries (LIBs) have been the best option for storage in recent years. The positive electrode materials for LIBs are usually inorganic materials such as cobalt, nickel, and manganese;[1] however, these are toxic and can contaminate water supplies and ecosystems. Utilizing redox-active organic molecules for sustainable energy storage devices has attracted significant attention owing to their potential low cost, low toxicity, and sustainability.[2–7] However, the dissolution of organic materials in liquid electrolytes results in a fast capacity decay, which has limited their practical application.

Our research group has sought to lower the solubility of redox-active tetrathiafulvalene (TTF) analogs[8] by increasing the size and planarity of the molecules and intermolecular interactions.[9–18] Recently, we have successfully demonstrated the application of TTF bearing triphenylamines (TTF-4TPA, Fig. 1) as long-cycle-life electrodes for LIBs *via* the "in-cell polymerization" technique.[19] The most important point of the design was that polymers could be generated without

redox-inactive linkages since the TPA moieties could couple during the charging process with each other at the *para*-position carbon on the benzene rings. TTF-4TPA undergoes a fourteen-electron oxidation reaction during the initial charge process. In-cell polymerization takes place by coupling of radical species generated during the process, accompanied by an irreversible eight-proton release. When the polymerization is accomplished, the resulting polymer can exhibit a reversible six-electron redox reaction during the charge–discharge process. Therefore, the theoretical capacity of the monomer of TTF-4TPA was 319 mA h g^{-1} based on the assumption of fourteen-electron transfer reactions and 137 mA h g^{-1} for the polymer of TTF-4TPA based on the assumption of six-electron
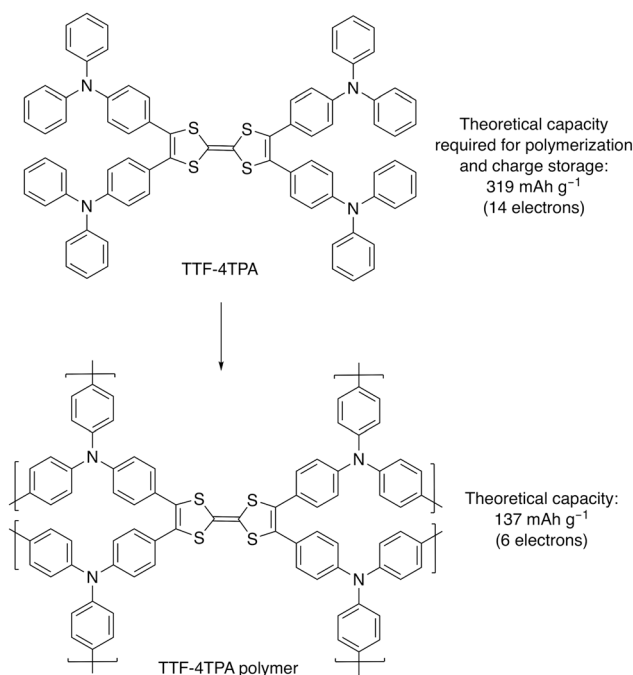
[a] Department of Applied Chemistry, Graduate School of Science and Engineering, Ehime University 3 Bunkyo-cho, Matsuyama 790-8577, Japan. E-mail: misaki.yohji.mx@ehime-u.ac.jp

[b] Research Unit for Development of Organic Superconductors, Ehime University 2-5 Bunkyo-cho, Matsuyama 790-8577, Japan

[c] Research Institute of Electrochemical Energy, National Institute of Advanced Industrial Science and Technology (AIST) 1-8-31 Midorigaoka, Ikeda, Osaka 563-8577, Japan

† Electronic supplementary information (ESI) available. CCDC 2223557–2223558. For ESI and crystallographic data in CIF or other electronic format see DOI: https://doi.org/10.1039/d3nj00289f

Fig. 1 Chemical structures and the theoretical capacities of TTF-4TPA and TTF-4TPA polymer.

transfer reactions. Furthermore, the in-cell polymerization of TTF-4TPA was almost complete during the first charge, and the utilization ratio of the obtained polymer was approximately 100%. However, compared to the capacity of general LIBs based on inorganic electrode materials, the capacity of the TTF-4TPA polymer was low (~ 150 mA h g^{-1}). Consequently, the synthesis of novel redox-active organic molecules with a capacity higher than that of TTF-4TPA and with a long cycle life is highly desirable.

In this paper, we designed compounds **1** and **2**, that is, benzene-fused TTF (Bz-TTF) having lower solubility than that of TTF-bearing TPA or *N*-methyldiphenylamine moieties (Fig. 2). The theoretical capacities of the monomer and polymer of **1** are 289 (eight electrons) and 145 mA h g^{-1} (four electrons) and those of **2** are 261 (six electrons) and 174 mA h g^{-1} (four electrons), respectively.

Compounds **1** and **2** were synthesized *via* a direct Pd-catalyzed C–H arylation of TTFs that has been previously reported[20–22] (Scheme 1). Bz-TTF was reacted with 4-bromotri-phenylamine in the presence of the Pd(OAc)$_2$/P^{t}Bu$_3$ system to produce **1** in 80% yield. Compound **2** was synthesized using the same procedure, and was obtained in an 82% yield.

Single crystals of **1** and **2**, suitable for single-crystal X-ray structure analysis, were obtained *via* the slow evaporation of the solvents from a toluene/ethyl acetate solution and dichloro-methane/^{n}hexane solution, respectively, at 25 °C. The crystals of **1** and **2** belonged to the triclinic ($P\bar{1}$) and monoclinic ($P2_1/c$) space groups, respectively (Table S1, ESI†). There was one crystallographically independent molecule for **1** and **2**. Fig. 3 and Fig. S1 (ESI†) show the molecular structures of **1** and **2**, respectively. The Bz-TTF core of **1** was slightly bent with the folding angle of the 1,3-dithiole ring along the S1–S2 axis being 17.0°. The two bulky TPA moieties on the 1,3-dithiole ring were twisted from the TTF core with dihedral angles of 41.0° (plane A–plane B) and 53.2° (plane A–plane C). The PXRD patterns of the powder **1** were characterized by the presence of sharp peaks at positions similar to those of the simulated one. On the other hand, powder **2** might have some differences from the single crystal phase (Fig S5, ESI†).

The redox properties of **1** and **2** were examined by cyclic voltammetry (CV) in a benzonitrile/carbon disulfide (1/1, v/v)
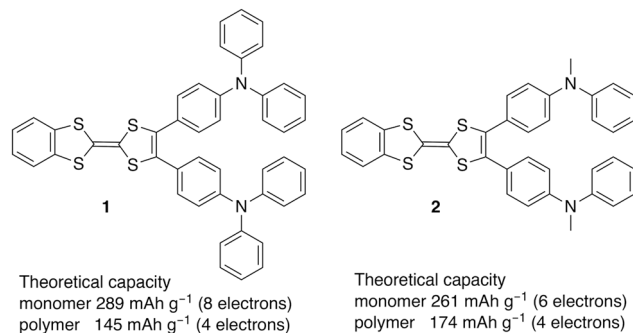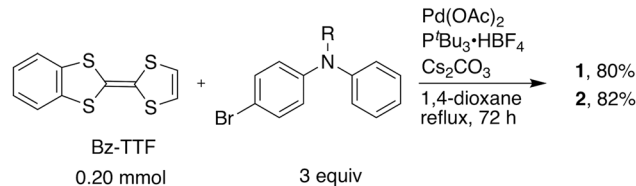
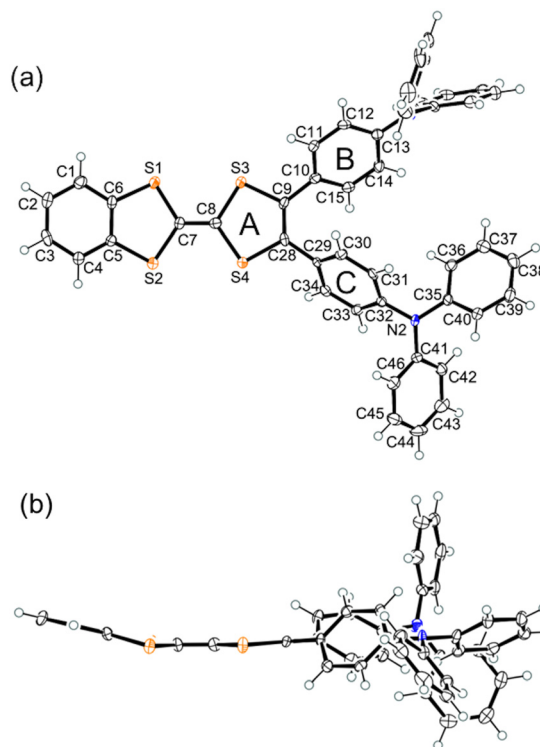Scheme 1   Synthesis of compounds **1** and **2**.

Fig. 3   (a) Top and (b) side views of the ORTEP drawings for **1**. Ellipsoids displayed at 50% probability.

solution. Compound **1** exhibited two pairs of redox waves in the −0.1 to +0.5 V range (*vs.* Fc/Fc$^+$, where Fc denotes ferrocene) derived from the TTF moiety. The redox potentials of **1** ($E_1 = 0.12$ V and $E_2 = 0.40$ V) are similar values to other arylated TTFs with electron-donating substituents (for example, $E_1 = -0.11$ V and $E_2 = 0.34$ V for tetrasubstituted TTF by 4-methoxybenzene).[20] In addition, a few extra oxidation and reduction waves derived from the redox reaction of the TPA moiety were also observed at significantly positive potentials around +0.6 V (Fig. 4 and Fig. S6a, ESI†), which were similar to previously reported donor–acceptor molecules bearing TPA moieties.[23] Compound **2** also exhibited two pairs of redox waves derived from the Bz-TTF moiety in addition to a few additional oxidation and reduction waves derived from the redox reaction of the TPA moiety (Fig. S6b and c, ESI†). Significantly, the oxidation and reduction currents of **1** and **2** increased with an increase in the number of CV cycles. These results were similar to those of TTF-TPA, thereby indicating the formation of a polymer on the electrode.
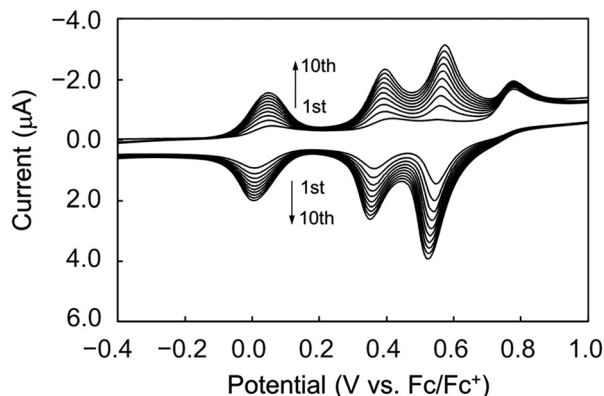
Fig. 2   Chemical structures and theoretical capacities of compounds **1** and **2**.

Fig. 4 Repeating CV cycles of **1** (3.0×10^{-4} M) at a scan rate of 50 mV s^{-1} in a benzonitrile–carbon disulfide (1/1, v/v) solution containing ^{n}Bu$_4$NPF$_6$ (0.1 M).

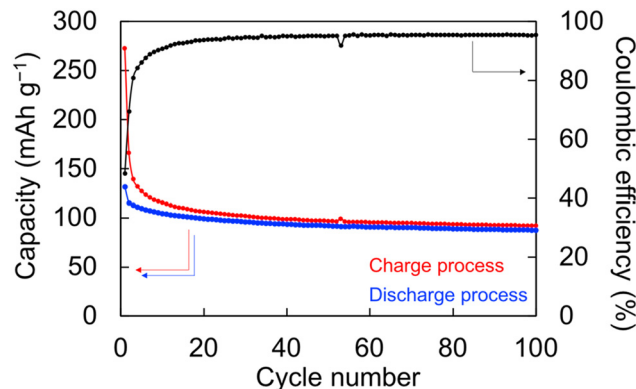The charge–discharge performances of the two different coin cells **1**/Li and **2**/Li composed of 10 wt% of **1** and **2**, respectively, as the active materials were then investigated. The charge and discharge capacities for the **1**/Li cell in the first cycle were 272 and 132 mA h g^{-1} (Fig. 5), respectively, which were over 90% of the theoretical capacity based on the assumption of eight-electron transfer reactions (289 mA h g^{-1}) and four-electron transfer reactions (145 mA h g^{-1}), respectively.[24] The charge processes from the third to the fifth cycles and the discharge processes from the second to the fifth cycles were observed with good reversibility. These results indicated that complete polymerization was achieved during the first two charge processes. Furthermore, the **1**/Li cell exhibited a stable cycle life (Fig. 6). For example, the capacity after 100 cycles was 81% of that in the fifth cycle. These results were similar to those of TTF-4TPA.[19] The rate performance of the in-cell polymerized **1**/Li was investigated at different current densities of 0.1–20 A g^{-1} and in a voltage range of 2.5–4.3 V after 10 cycles. The electrode containing 50 wt% of **1** also showed similar performances, exhibiting approximately 51% of the capacity of the electrodes containing 10 wt% of **1** (Fig. S7, ESI†).[25]
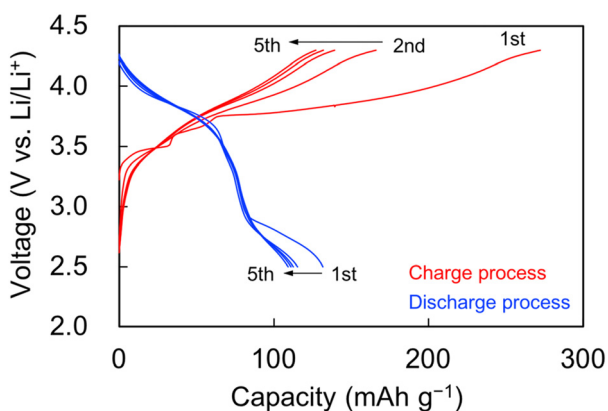

Fig. 5 Galvanostatic charge–discharge curves of the **1**/Li cell at current densities of 40 mA g^{-1} (charge) and 100 mA g^{-1} (discharge).

Fig. 6 Cyclic trend and Coulombic efficiency in the charge and discharge capacities of the **1**/Li cell.
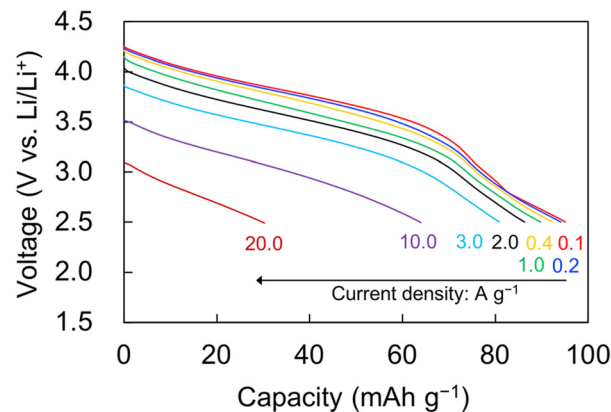

Fig. 7 Selected discharge profiles of the **1**/Li cell at different current densities.

The selected discharge curves showed a slight decrease in potential at high current densities (Fig. 7). For example, when the current rate increased from 0.1 to 3.0 A g^{-1}, the capacity slightly decreased from 95 to 81 mA h g^{-1}. Even at current rates of 10 and 20 A g^{-1}, the **1**/Li cell had capacity retentions of 64 and 30 mA h g^{-1}, respectively.

The charge capacity for the **2**/Li cell in the first cycle was 284 mA h g^{-1}, which was over 100% of the theoretical capacity based on the assumption of six-electron transfer reactions (261 mA h g^{-1}) (Fig. S8a, ESI†). Furthermore, the discharge capacity in the first cycle was 127 mA h g^{-1}, which was 73% of the theoretical capacity based on the assumption of four-electron transfer reactions (174 mA h g^{-1}). The charge capacities from the second to the fifth cycles and the discharge capacities from the first to the fifth cycles gradually decreased. The cyclic trend revealed that the capacity remained unstable until 35 cycles (Fig. S8b, ESI†). These results indicated that the polymerization of **2** slowly proceeded and **2** was partially soluble, probably since it has only two polymerization sites.[26]

After in-cell polymerization was completed, the Coulombic efficiencies of both **1** and **2**/cells were sufficiently high, which was also observed with TTF-4TPA (Fig. 6 and Fig. S7b, ESI†).[19,27] The charge–discharge parameters for the rechargeable batteries

using **1** and **2** are summarized in Table S2 (ESI†). The average voltages for the first discharge cycle for **1** and **2** were 3.37 V (*vs.* Li/Li$^+$) and 3.24 V for **2**, respectively, and the energy densities for the first discharge cycle for **1** and **2** were 445 mW h g^{-1} and 411 mW h g^{-1}, respectively. The utilization ratio of the obtained polymer was approximately 78% at the 3rd cycle for **1** and 47% at the 35th cycle for **2** and during the charge–discharge processes.

Our group has previously proposed the redox and polymerization processes for TTF-4TPA to rationalize in-cell polymerization.[19] Because of the high resemblance between the properties of **1** and TTF-4TPA, it was speculated that the redox and polymerization processes of **1** proceeded according to Scheme S1 (ESI†), where neutral **1** might repeat the redox and polymerization reactions to form the tetracation of polymer-**1** *via* eight-electron redox reactions. After generating the tetracation of polymer-**1**, it may be changed to the neutral form of polymer-**1**, *via* a four-electron redox reduction reaction. In addition, we confirmed the "in-cell polymerization" experimentally. As for the cell electrode before the charge–discharge processes, the orange solution was obtained by washing the cell electrodes using 5 mL of carbon disulfide (CS$_2$) (Fig. S9a, ESI†). By the analysis of ^{1}H NMR after evaporation of CS$_2$, monomer **1** was detected (Fig. S10a, ESI†). In sharp contrast, the cell electrode after the charge–discharge processes gave a colorless solution obtained by the same operation (Fig. S9b, ESI†), and monomer **1** was not observed at all from the ^{1}H NMR spectra after evaporation of CS$_2$ (Fig. S10b, ESI†). These results indicate that the polymerization proceeded in the cell during the charge–discharge processes. Although the acidity of the medium might increase during the polymerization process due to the deprotonation processes, it could be found that the charge–discharge process was not affected by the desorbed protons under this condition.

Conclusions

We designed compounds **1** and **2**, which could prolong the cycle life of LIBs *via* the "in-cell polymerization" technique. Compounds **1** and **2** were successfully synthesized using easy-handled Pd-catalyzed direct C–H arylation. The structure of **1** and **2** was determined by X-ray crystallography. Excellent electrochemical performance of the **1**/Li cell was demonstrated by the Li cell comprising **1** with a high capacity of 132 mA h g^{-1} in the first cycle, a high discharge voltage of 3.37 V, a stable cycle life of 81% after 100 cycles for that in the 5th cycle, and a high rate performance, that is, the capacity at a current density of 3.0 A g^{-1} was 81% of that at a current density of 0.1 A g^{-1}. On the other hand, the in-cell polymerization of **2** would proceed slowly probably because **2** has only two polymerization sites. As a result, **2** might be somewhat soluble to the electrolyte and the capacity was not stable until 35 cycles in the cyclic trend.

Author contributions

Y. Misaki directed the project. A. Yoshimura, M. Yoshinouchi, K. Hemmi, Y. Aso, and R. Utsumi performed the synthesis, CV, and XRD measurement. A. Yoshimura, Y. Aso, and T. Shirahata performed a single X-ray structural analysis. M. Yao examined the cell performance. A. Yoshimura wrote the manuscript draft. A. Yoshimura, T. Shirahata, M. Yao, and Y. Misaki revised the manuscript. All authors discussed the results. A. Yoshimura, T. Shirahata, and Y. Misaki raised research funds.

Conflicts of interest

There are no conflicts to declare.

Acknowledgements

References

1 M. Armand and J.-M. Tarascon, *Nature*, 2008, **451**, 652.
2 Y. Misaki, in *Functional Materials: Advances and Applications in Energy Storage and Conversion*, ed. T. Naito, Pan Stanford Publishing, Singapore, 2019, p. 205.
3 Y. Liang, Z. Tao and J. Chen, *Adv. Energy Mater.*, 2012, **2**, 742.
4 Q. Deng, Z. Luo, R. Yang and J. Li, *ACS Sustainable Chem. Eng.*, 2020, **8**, 15445.
5 M. Souto, K. Strutyński, M. Melle-Franco and J. Rocha, *Chem. – Eur. J.*, 2020, **26**, 10912.
6 K. Qin, J. Huang, K. Holguin and C. Luo, *Energy Environ. Sci.*, 2020, **13**, 3950.
7 Q. Yu, W. Tang, Y. Hu, J. Gao, M. Wang, S. Liu, H. Lai, L. Xu and C. Fan, *Chem. Eng. J.*, 2021, **415**, 128509.
8 TTF derivatives are superior active materials in terms of their theoretical capacities and redox potentials. See ref. 2.
9 Y. Inatomi, N. Hojo, T. Yamamoto, S. Watanabe and Y. Misaki, *ChemPlusChem*, 2012, **77**, 973.
10 M. Kato, D. Ogi, M. Yao and Y. Misaki, *Chem. Lett.*, 2013, **42**, 1556.
11 M. Kato, K. Senoo, M. Yao and Y. Misaki, *J. Mater. Chem. A*, 2014, **2**, 6747.
12 D. Ogi, Y. Fujita, M. Kato, T. Yamauchi, T. Shirahata, M. Yao and Y. Misaki, *Eur. J. Org. Chem.*, 2019, 2725.
13 T. Yamauchi, M. Kato, T. Shirahata, M. Yao and Y. Misaki, *Chem. Lett.*, 2019, **48**, 1507.

14 Y. Misaki, S. Noda, M. Kato, T. Yamauchi, T. Oshima, A. Yoshimura, T. Shirahata and M. Yao, *ChemSusChem*, 2020, **13**, 2312.

15 T. Yamauchi, W. Hirabayashi, A. Yoshimura, M. Yao and Y. Misaki, *Bull. Chem. Soc. Jpn.*, 2021, **94**, 44.

16 T. Oshima, A. Sasaki, T. Yamauchi, A. Yoshimura, T. Shirahata, M. Yao and Y. Misaki, *Chem. Lett.*, 2021, **50**, 1164.

17 T. Yamauchi, T. Kubo, A. Fujioka, A. Yoshimura, T. Shirahata, H. Miyamoto, M. Yao and Y. Misaki, *Bull. Chem. Soc. Jpn.*, 2021, **94**, 1940.

18 Y. Kawasaki, R. Sakakibara, M. Fujisaki, M. Yamashita, A. Yoshimura, T. Shirahata, M. Yao and Y. Misaki, *Bull. Chem. Soc. Jpn.*, 2021, **94**, 1059.

19 A. Yoshimura, K. Hemmi, H. Moriwaki, R. Sakakibara, H. Kimura, Y. Aso, N. Kinoshita, R. Suizu, T. Shirahata, M. Yao, H. Yorimitsu, K. Awaga and Y. Misaki, *ACS Appl. Mater. Interfaces*, 2022, **14**, 35978.

20 Y. Mitamura, H. Yorimitsu, K. Oshima and A. Osuka, *Chem. Sci.*, 2011, **2**, 2017.

21 H. Yorimitsu, A. Yoshimura and Y. Misaki, *Synthesis*, 2020, 3326.

22 A. Yoshimura and Y. Misaki, *Chem. Rec.*, 2021, **21**, 3520.

23 M.-K. Leung, M.-Y. Chou, Y. O. Su, C. L. Chiang, H.-L. Chen, C. F. Yang, C.-C. Yang, C.-C. Lin and H.-T. Chen, *Org. Lett.*, 2003, **5**, 839.

24 The capacities were 67 and 72 mA h g^{-1} for compounds **1** and **2**, respectively, when they are calculated considering the six molecules of PF_6^- involved in the redox reaction of polymers of **1** and **2**.

25 The capacities at the 2nd cycle were compared.

26 Although we cannot say for certain because the polymerization does not take place in the crystal, we speculate that a longer distance of p-position carbon on the benzene rings of **2** compared to those of **1** and TTF-4TPA in single crystals may be considered one of the reasons for the slow polymerization (Fig. S4, ESI†).

27 The Coulombic efficiency before completing the polymerization remains low because the polymerization proceeded using many electrons.